

Supporting Information

Time-Resolved Imaging of High Mass Proteins and Metastable Fragments Using Matrix-Assisted Laser Desorption/Ionization, Axial Time-of-Flight Mass Spectrometry, and TPX3CAM

Anjusha Mathew¹, Joel D. Keelor², Gert B. Eijkel¹, Ian G. M. Anthony¹, Jingming Long², Jord Prangma², Ron M. A. Heeren^{1*} and Shane R. Ellis^{1,3*}

¹Maastricht MultiModal Molecular Imaging (M4i) Institute, Division of Imaging Mass Spectrometry (IMS), Maastricht University, 6229 ER Maastricht, The Netherlands

²Amsterdam Scientific Instruments (ASI), Science Park 106, 1098 XG Amsterdam, The Netherlands

³Molecular Horizons and School of Chemistry and Molecular Bioscience, University of Wollongong, NSW 2522, Wollongong, Australia

*To whom correspondence should be addressed:

r.heeren@maastrichtuniversity.nl

sellis@uow.edu.au

Table of contents

Table S1 List of the data acquisition parameters.....	S-3
Figure S1 TOF to m/z conversion curve.....	S-4
Figure S2 Pixel cluster histogram of IgG ions.....	S-5
Figure S3 TOT distribution of IgG ions.....	S-6
Figure S4 Pixel cluster histogram of IgM ions.....	S-7
Figure S5 Pixel cluster histogram of ions generated from Bruker peptide calibration standard II.....	S-8
Figure S6 m/z resolved TPX3 images corresponding to the main peaks of Bruker protein calibration standard II mass spectrum.....	S-9
Figure S7 Pixel cluster histograms of the precursor insulin chain B $[M+H]^{1+}$ ions and metastable neutrals formed prior to the deflector.....	S-10
Figure S8 TOF spectra of the precursor insulin chain B $[M+H]^{1+}$ ions and metastable neutrals formed prior to the deflector.....	S-11
Figure S9 Axial TPX3 images and TOF spectra of the precursor insulin chain B $[M+H]^{1+}$ ions and metastable neutrals at different reflectron voltages.....	S-12

Table S1. List of the data acquisition parameters

Parameter	Figure 2 (fg)	Figure 3 (fgM)	Figure 4a & b (Peptide std II)	Figure 4e & f (Protein std II)	Figure 5 (Insulin chain B)	Figure S9 (Insulin chain B)
Number of laser shots/measurement cycles	5000	5000	1000	1000	5000	5000
Laser repetition rate (Hz)	100	100	100	100	10	10
Laser power (%)	50	70	30	50	30	30
Target plate voltage (kV)	25	25	25	25	25	25
Second plate voltage (kV)	21	21	23.6	23.1	22.45	22.45
Lens voltage (kV)	12	12	7	6	6	6
Reflectron voltage (kV)	0	0	0	0	0, 0 and 19.5 (Scenario 1, 2 and 3)	0, 5, 10, 15, 20, 25
Pulsed ion extraction (PIE, ns)	500	2000	0	500	0	0
Matrix suppression deflection (Da)	15000	100000	700	10000	1000	1000
Global attenuator offset (%)	65	65	45	65	45	45
Attenuator offset (%)	15	15	25	15	25	25
Focus offset (%)	0	0	0	0	0	0
Focus range (%)	100	100	100	100	100	100
Focus position (%)	33	33	33	33	33	33
x-deflection voltage (V)	0	0	0	0	0, -55 and -55 (Scenario 1, 2 and 3)	-55
y-deflection voltage (V)	0	0	0	0	0, -65 and -65 (Scenario 1, 2 and 3)	-70
Linear MCP front plate voltage (V)	-2150	-2600	-2100	-2200	-2100	-2100
Linear MCP back plate voltage (V)	-600	-600	-600	-600	-600	-600
Phosphor screen voltage (V)	5000	5000	5000	5000	5000	5000
TPX3CAM f-stop value	0.95	0.95	0.95	0.95	0.95	0.95
DG535 channel A pulse width (delay for TPX3, μ s)	75	125	20	20	20	20
DG535 channel B pulse width (measurement window for TPX3, μ s)	1000	2000	150	500	100	100
DG535 channel C pulse width (delay for internal TDC SPDR, μ s)	75	125	20	20	20	20
DG535 channel D pulse width (measurement window of internal TDC SPDR, μ s)	100	100	100	100	100	100

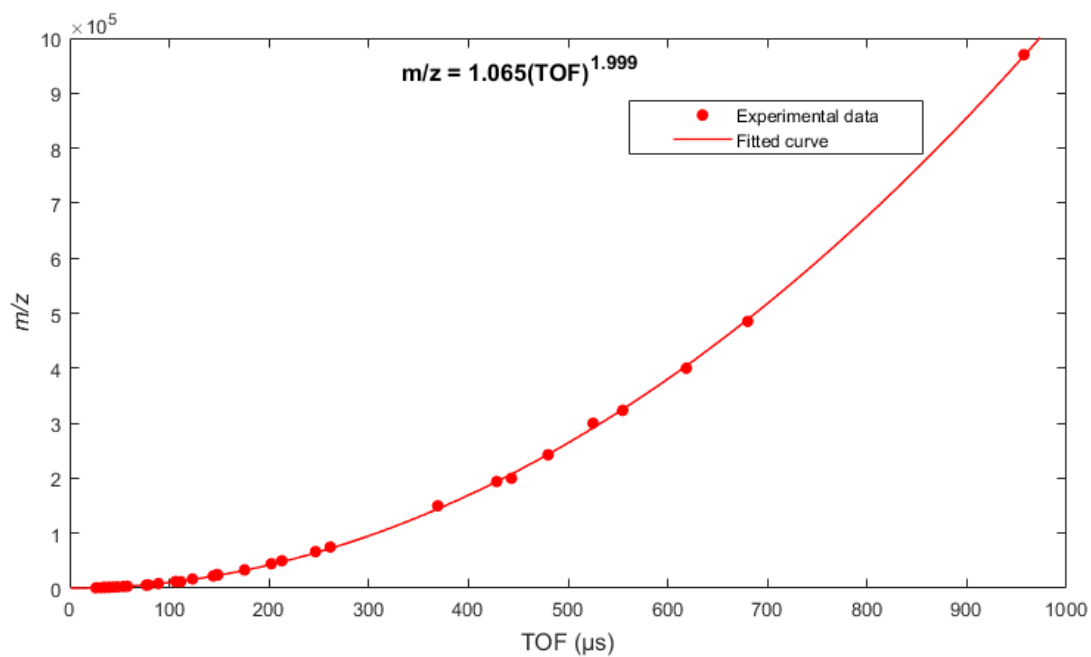


Figure S1. TOF to m/z conversion curve plotted using 10 samples that encompasses an m/z range from 750 to 970,000 Da. All the TOF data were acquired using an initial acceleration voltage (target plate voltage) of 25 kV.

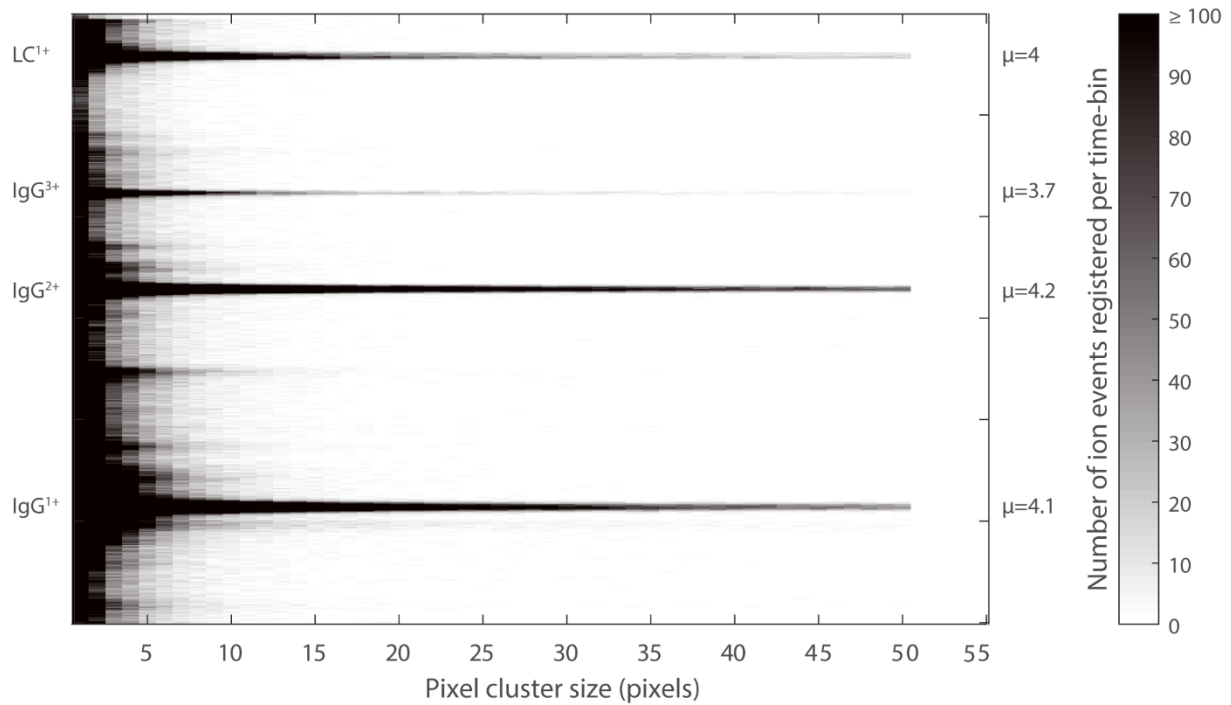


Figure S2. Distribution of pixel cluster area (in pixels) of LC¹⁺, IgG³⁺, IgG²⁺ and IgG¹⁺ ions, and corresponds to the data shown in Figure 2. A time-bin size of 500 ns was used for the generation of the histogram. μ is the average pixel cluster size that is calculated by $\frac{\sum_{i=1}^k (i \times N_i)}{\sum_{i=1}^k N_i}$, where i =pixel cluster size (in pixels), N_i =number of ion events with pixel cluster size of 'i', and k = maximum pixel cluster size (in pixels).

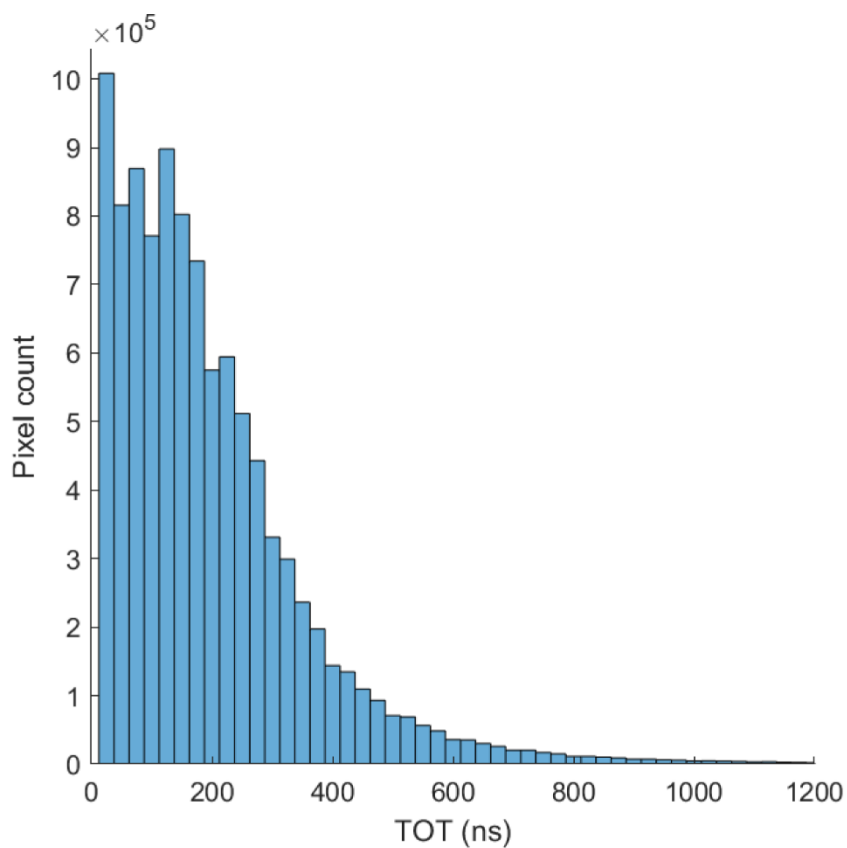


Figure S3. TOT distribution of the TPX3 pixels triggered by IgG ions (m/z range: 25-150 kDa), and corresponds to the data shown in Figure 2. A time-bin size of 25 ns was used for the generation of the histogram.

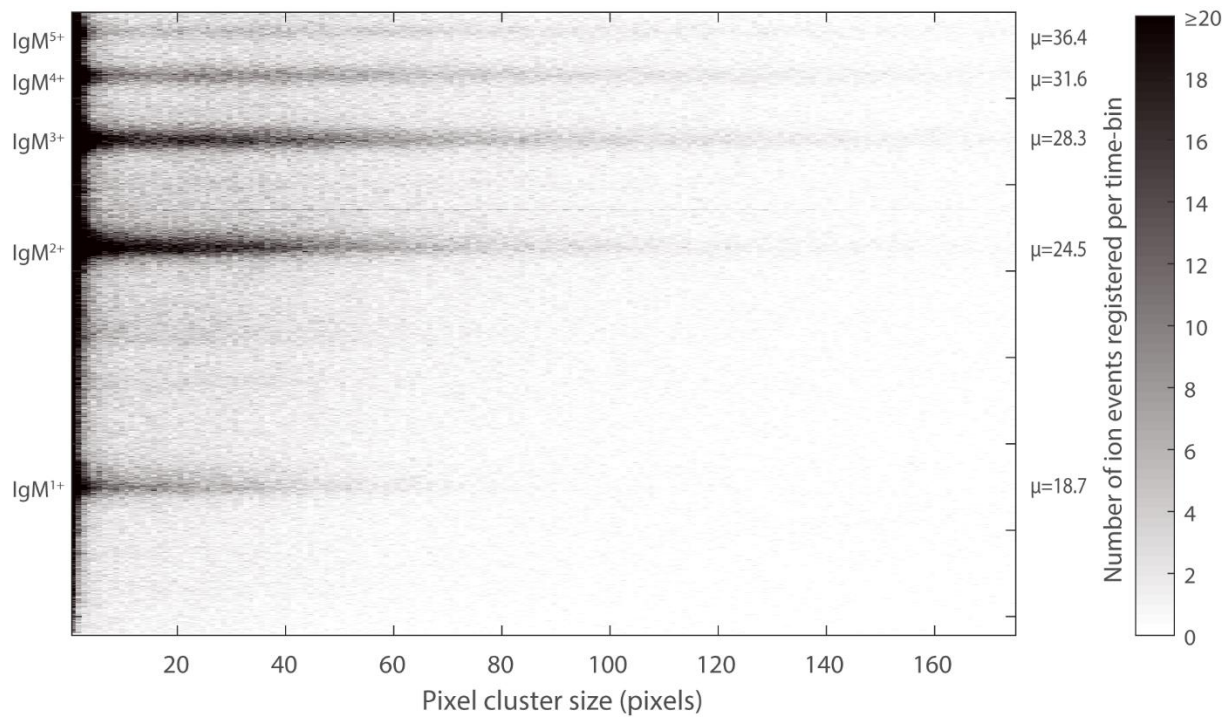


Figure S4. Distribution of pixel cluster area (in pixels) of IgM 1⁺-5⁺ ions, and corresponds to the data shown in Figure 3. A time-bin size of 500 ns was used for the generation of the histogram. μ is the average pixel cluster size that is calculated as previously described (Figure S2).

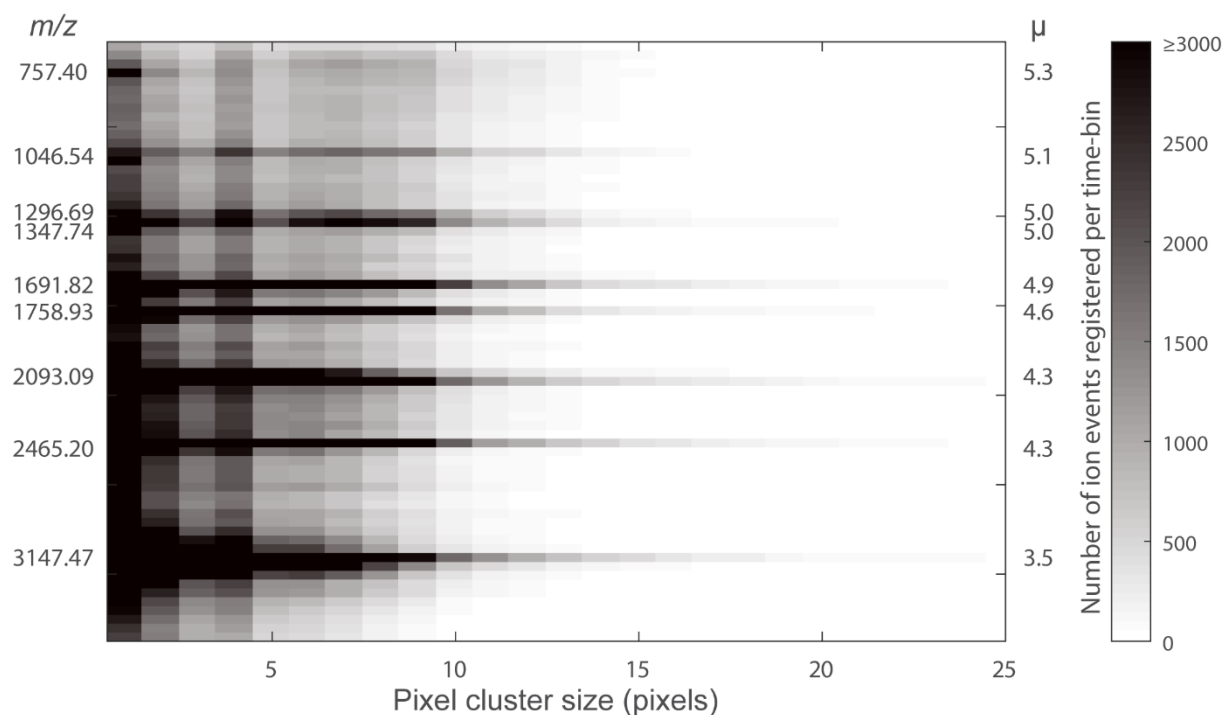


Figure S5. Distribution of pixel cluster area (in pixels) of the ions generated from Bruker peptide calibration standard II (m/z range: 700-3200 Da), and corresponds to data shown in Figure 4a and b. A time-bin size of 500 ns was used for the generation of the histogram. μ is the average pixel cluster size that is calculated as previously described (Figure S2).

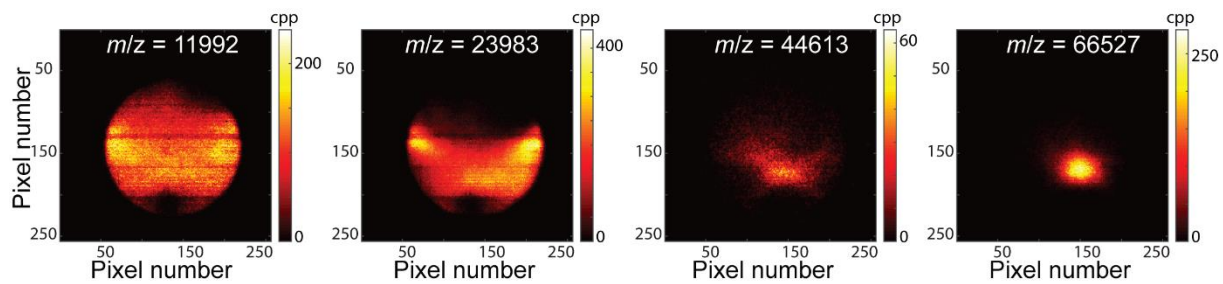


Figure S6. m/z resolved TPX3 images of Trypsinogen²⁺ ($m/z=11,992$), Trypsinogen¹⁺ ($m/z=23,983$), Protein A¹⁺ ($m/z=44,613$) and BSA¹⁺ ($m/z=66,527$) from Bruker protein calibration standard II, and generated from data shown in Figure 4e and f by the accumulation of 1000 laser shots (cpp=counts per pixel).

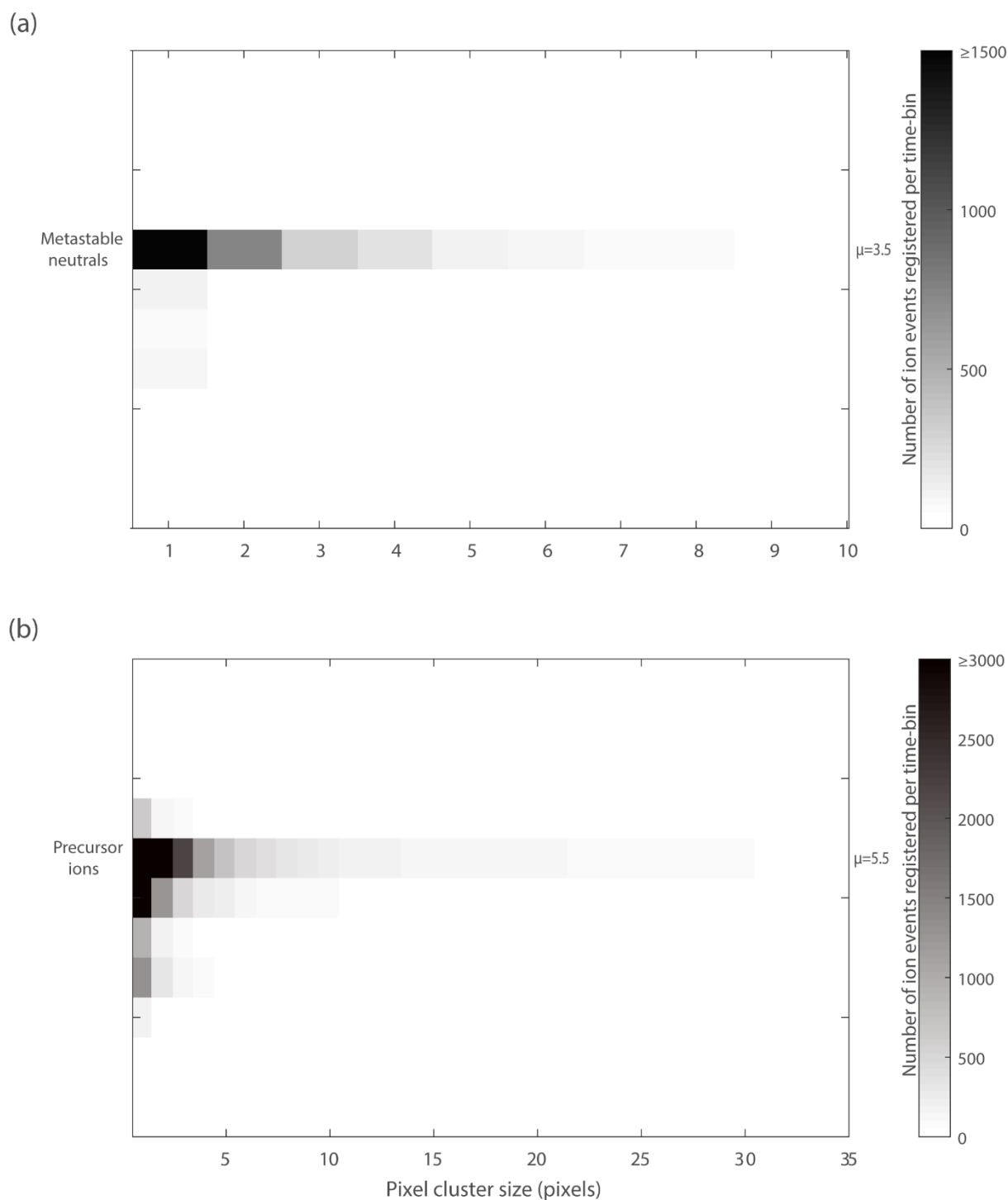


Figure S7. Distribution of pixel cluster area (in pixels) of metastable neutrals formed in between the source and deflector (a) and precursor insulin chain B $[M+H]^{1+}$ ions (b), and corresponds to data shown in Figure 5b, e and h (Scenario 2). A time-bin size of 500 ns was used for the generation of the histogram. μ is the average pixel cluster size that is calculated as previously described (Figure S2).

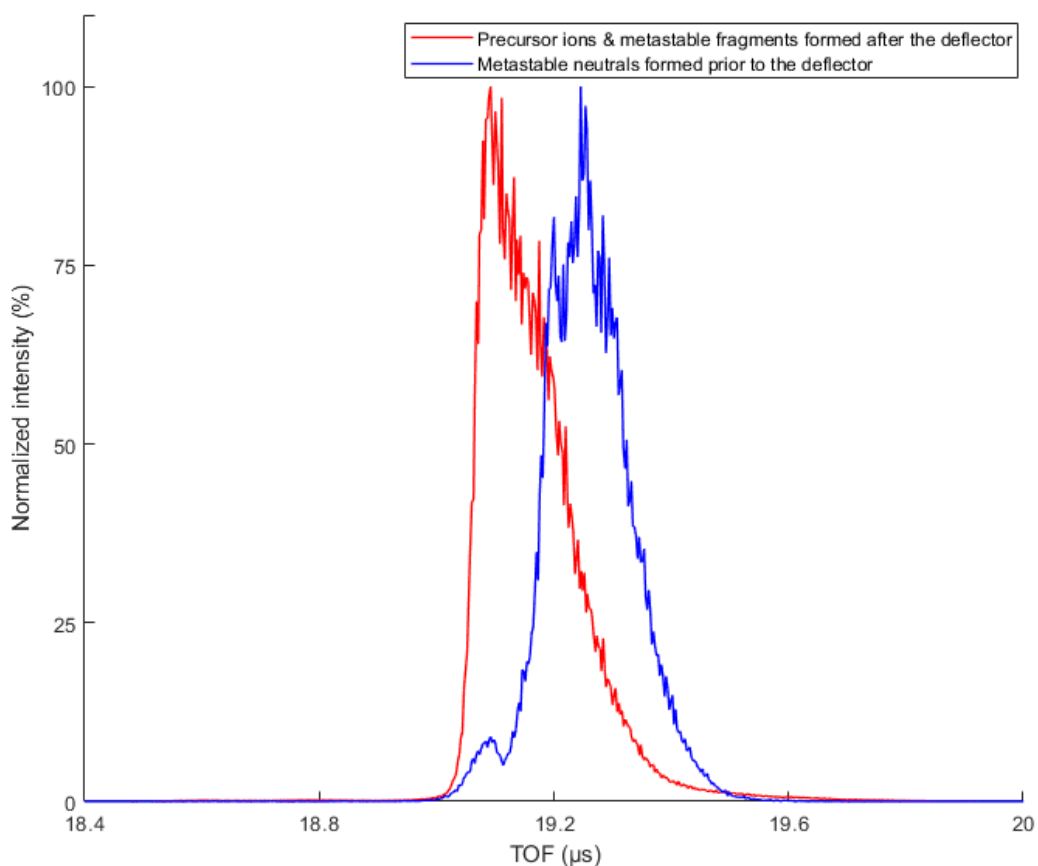


Figure S8. TOF spectra correspond to the intact insulin chain B $[M+H]^{1+}$ ions (red trace) and metastable neutrals formed prior to the deflector (blue trace). Data was acquired with deflector voltage on and reflectron voltage off (Scenario 2 in Figure 5). Note that the intensities in both cases are normalized to their respective maximum for the better comparison and visualization of the TOF spectra.

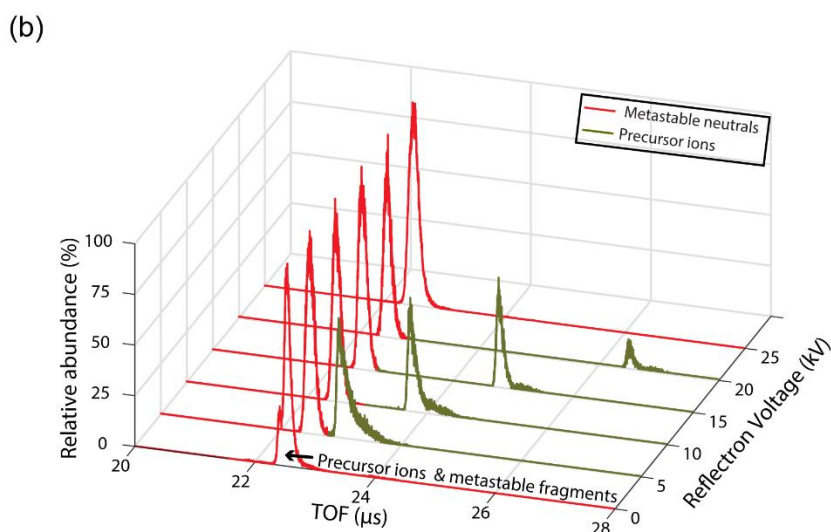
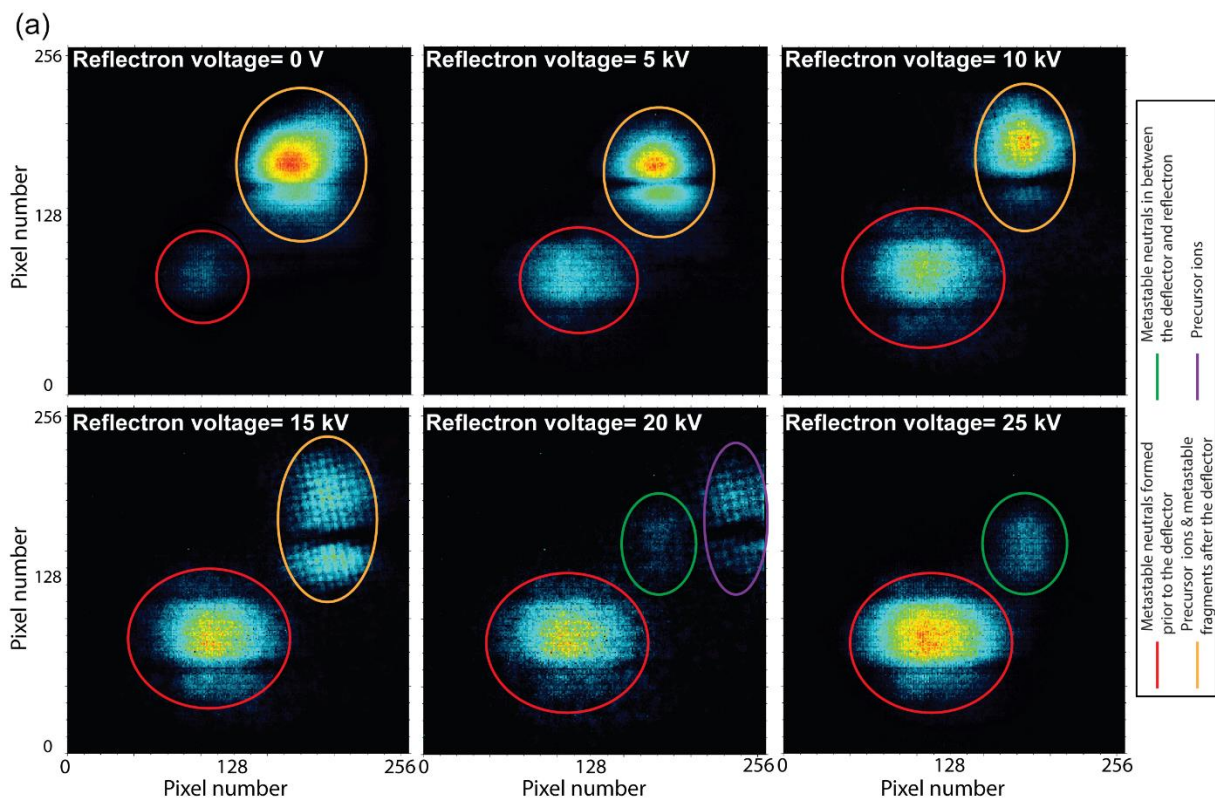


Figure S9. Evolution of the (a) total ion TPX3 images and (b) linear TPX3 detector TOF spectra with an increase in the reflectron voltage (a deflection voltage is also applied). Note that the intensities are normalized to their respective maximum for all the TOF spectra. The data acquisition parameters are listed in Table S1.